Synthesis and Behavior of the Polymer Covering on a Solid Surface. 3. Morphology and Mechanism of Formation of Grafted Polystyrene Layers on the Glass Surface

Igor Luzinov,[†] Serhiy Minko,*[,‡] Volodimir Senkovsky, and Andriy Voronov[§]

Lviv Department of Physical Chemistry Institute, National Academy of Sciences, 3a Naukova, Lviv, 290053, Ukraine

Sabine Hild, Othmar Marti, and Wolfgang Wilke

Department of Experimental Physics, University of Ulm, D-89069 Ulm, Germany

Received September 23, 1997; Revised Manuscript Received March 9, 1998

ABSTRACT: Polystyrene films have been grafted by radical polymerization in situ on the surface of glass slides. The morphology of these films resulting from different grafting temperatures has been investigated by both the contact angle method and scanning probe microscopy with respect to the grafting time. At a grafting density regime where the theory proposes the existence of a homogeneous layer, the formation of island structures of grafted polymer with a size substantially higher than expected by the theory has been observed. Overshot polymer structures of large sizes are created. The amount of grafted polymer is substantially higher than that predicted from the conception of monolayer covering. The grafting layer becomes impermeable for water only at a high amount of grafted polymer, which corresponds to the multilayer structure of the coating. We suggested a mechanism for the grafting process that included at least three stages: (a) first, a brushlike polymer layer is formed; (b) subsequently, a second layer of ungrafted chains is created in the regime when excess chains are forced out from the first layer; (c) big polymer clusters, with an average size of 100−200 nm due to gel polymerization in the clusters, formed in the force out regime.

Introduction

Since surface covering with polymers is feasible, thin polymer layers, i.e., a monolayer or multilayers, become of great interest, because this allows to control many surface properties such as wetting, colloidal stability (for powders), adhesion, lubrication, anisotropic conductivity, piezochromic effect, etc. There are several main methods to generate these layers: polymer adsorption, grafting on the solid surface, the spin coating method, and the Langmuir−Blodgett technique. Only by grafting in situ are the synthesis of a polymer on a substrate and the simultaneous layer formation processes possible. In contrast to other methods, when a coating is formed from the previously prepared polymer, the grafting enables one to create a layer and synthesize a polymer simultaneously that could have some specific interesting possibilities to tailor coatings. The density of grafting can be changed in a wide range from single chains on the surface to high density of grafting even to the situation when an excess of polymer is overshot. So far, to our knowledge, despite the high number of papers about grafting from the solid substrate, there are few works about the morphology of grafted in situ layers.

The polymer chains grafted on the solid substrate belong to the class of tethered polymer chains. The end-attaching to the solid substrate chains was a subject for numerous theoretical and experimental research (see, e.g., some reviews[1−5]). Recently, atomic force microscopy was successfully applied to study the properties of end-attaching chains under conditions of good and poor solvents.[6−10]

In this paper we will study the grafting process on the glass surface by investigation of the polymer layer morphology with scanning probe microscopy (SPM) and the contact angle method. For this investigations the solvent is removed after grafting and the morphology of the dry polymer layer is examined. The structures of the dry polymer layer can be considered as formed under the conditions of a poor solvent. The polymer brushes in such layers have been analyzed in theoretical studies. In particular, Yeung et al.[11] use the random phase approximation and numerical mean field analysis. For sufficiently poor solvents they found that the laterally homogeneous grafted layer is linearly unstable to fluctuations tangential to the grafting plane. It forms a dimpled surface in which the depth and the separation of the dimples depend on chain length, solvent quality and grafting density. This instability is caused by the competition of attractive forces between the molecular chains and the grafting constraints. For small and large values of the parameter γ, which describes the stretching of the chains in the direction normal to the chains' lateral expansion, different features of the dimples have been found. At small γ, the layer forms a dimpled surface where the distance between dimples is on the order of the radius of gyration of the chain in Θ solvent (R_g^{Θ}) and the height of the dimples is in the order of the layer thickness. At large γ, the instability is restricted to a region near to the top of the grafted layer and the distance between the dimples is larger than R_g^{Θ}. A similar behavior for grafted layers has been found due

* To whom correspondence should be addressed.
[†] Current address: Centre for Education and Research on Macromolecules, University of Liege, Sart-Tilman B6, 4000 Liege, Belgium.
[‡] Current address: Department of Experimental Physics, University of Ulm, Albert-Einstein-Allee 11, D-89069, Germany.
[§] Current address: Institute Charles Sadron, 6 rue Boussingault, 67083 Strasbourg, France.

S0024-9297(97)01413-7 CCC: $15.00
Published on Web 05/23/1998

to scaling analyses performed by Tang and Szleifer.[12] They obtain three regimes of possible structures: mushrooms, clusters, and layers.

First experimental results on these structural regimes are presented by Stamm et al.[13] They studied the adsorption of polystyrene end-functionalized by short polybutadiene blocks with urazole groups on silicon wafers. In this work the different structures, individual clusters of grafted polymer chains, dimples, and laterally homogeneous layers, are identified by SPM technique for saturated adsorbed layers of different molecular weight specimens of the polymer. For a low density of grafting (0.002 chains/nm^2), the observed domains have an average radius of 25 nm and height of 4 nm. In contrast, the calculated value of R_g^Θ is 33 nm. The correlation indicates that the domains observed are isolated clusters of polymer chains (mushrooms) consisting of approximately 12 chains. For a grafting density of 0.065 chains/nm^2, a dimpled structure has been observed. The dimples are about 40 nm wide and 3 nm high. The average distance between them is about 50 nm, and the calculated value of R_g^Θ is 10 nm. Consequently, the lateral distance between the dimples is larger than R_g^Θ, although the model has predicted a distance on the order of R_g^Θ. In theoretical studies the irregular spatial distribution of the clusters and even holes are explained by the fact that in experimental studies grafting density can be nonuniform. For large density grafting (0.21 chains/nm^2) a laterally homogeneous layer with a roughness of 0.3 nm can be observed. Therefore, it was shown experimentally, that at a high grafting density the coating becomes relatively smooth and homogeneous.

Uchida and Ikada[8] have studied the grafted polymer layers prepared by the polymerization of 2-(dimethylamino)ethyl methacrylate in situ on the poly(ethylene terephthalate) substrate. They obtained brushes in the wide range of molecular weight from 4400 to 150 000 (M_w) with approximately the same interchain distance on the surface about 1.7 nm, which was always lower than R_g^Θ. For such layers they observed SPM images underwater to be the same (laterally inhomogeneous structures—clusters) as in ref 13. Koutos[7] et al. have studied the chemically end-grafted polymer chains (thiol-terminated polystyrene on a gold substrate) with SPM underwater. At low coverage they found the individual collapsed polymer coils. At high grafted density they observed also the microphase separation of the polymer monolayers into globular clusters. They have shown that the sizes of the clusters satisfy the scaling laws.

In contrast to the above-mentioned work, we obtain the grafted layer by in situ radical polymerization on a solid surface in a wide range of grafted amounts of polystyrene. This enables us to exceed the amount of grafted chains corresponding to the saturated adsorption layer. The morphology of the layer in a "force out regime" is studied. For grafting on a solid substrate by the mechanism of radical polymerization "force out regime" means the situation when the surface is completely occupied by polymer brushes and no more grafted chains can grow on the surface. We may presume that the subsequent evolution of the process takes one of the following paths: (1) in the case of poor interaction between polymer and substrate the excess chains could be forced out from the surface; (2) in the case of strong polymer−surface interaction, e.g. chemical bonding to surface functional groups, the adhered free radicals are terminated by means of the chain transfer reaction, e.g. with monomer. Both possibilities result in the formation of unbounded polymer chains. Nevertheless, free polymer chains can be entangled with the grafted chains and, consequently, very slowly washed out from the grafted layer even at very good agitation of the reaction mixture. The excess polymer forms a "second polymer layer" on the surface. It was predicted theoretically and experimentally documented recently[14,15] that the first brushlike layer entropically repels the nongrafted chains. Because of this, the brushlike grafted layer becomes nonwettable by the same polymer chains. The ungrafted polymer layer spontaneously dewets the adhered layer. As a result, droplet structures are formed on the surface. The structure of such a heterogeneous surface depends on dewetting conditions and the molecular weight of the polymer. Consequently, one may presume that the morphology of the coating, which follows the grafting process in situ and subsequently forms in the dry film, is controlled by the above-mentioned mechanisms: (a) formation of laterally inhomogeneous grafted layer and (b) formation of droplet structures by ungrafted polymer on the surface of the first (grafted) layer. It is worth noting, that the process of multilayer coating formation compets with (c) the diffusion and washing out of ungrafted polymer by a solvent and the latter effects the thickness of the coating.

In this paper we experimentally proved this assumption and observed how the above-mentioned three factors affect the mechanism of coating formation. For the experiments, we employed the method of grafting by radical polymerization initiated from the polymer initiator (PI) adsorbed on the glass substrate. The aspects of PI adsorption are described in detail in previous papers.[16,17]

Experimental Section

Materials. As substrates *microscope slides* are used. They are rinsed with butyl acetate and heated at 500 °C. A definite amount of glass plates are milled, and the powder is used as reference for the evaluation of the grafted amount by pyrolysis. *Styrene* of reactive grade is distilled under reduced pressure with argon. *Polymer initiator* (PI)—a copolymer of peroxide group containing the monomer 5-*tert*-butyl-peroxy-5-methyl-1-hexen-3-yne and maleic anhydride (0.47:0.53 mol respectively) of $M_n = 2800$ and $M_w = 3200$—has been obtained from the Organic Chemistry Department of Lvivska Politechnica State University. Dicumene peroxide (DCP) and solvents (xylene and butyl acetate) of reactive grade are used as received.

Grafting. The grafting procedure is performed as described earlier.[18] The initiator is adhered to the glass surface due to PI adsorption from a 0.5% solution in butyl acetate. Afterward the surface is rinsed by the solvent five times to remove the surplus PI. Subsequently the sample is dried *in a vacuum* at room temperature. Glass plates and powder were covered with PI by use of the same conditions.

For grafting of polystyrene, the modified substrates, styrene, additional initiator DCP, and xylene are placed into the reaction vessel under nitrogen. With slight shaking, the mixture is heated in an oil bath to a given polymerization temperature for various times. After grafting, the plates or powders are rinsed six times in xylene to remove ungrafted polymer and dried *in a vacuum* at 60 °C. The amount of adsorbed PI and the amount of grafted polystyrene (PS) are evaluated by pyrolysis at 500 °C. The dried plates are investigated by scanning probe microscopy under ambient conditions and by scanning electron microscopy and tested with the contact angle method.

Contact Angle Measurements. By a microliter syringe a drop (0.001 mL) of double distilled water is put on the glass plate at 25 °C. Diameter (d) and height (h) of the drop are measured by a cathetometer. The contact angle is computed as $\tan(\Theta/2) = 2h/d$ with an accuracy of ± 1°. The fraction of the surface covered by the polymer can be evaluated by the Cassie equation:[19−21]

$$\cos(\Theta) = f_1 \cos(\Theta_1) + f_2 \cos(\Theta_2) + f_3 \cos(\Theta_3),$$
$$f_1 + f_2 + f_3 = 1 \quad (1)$$

where Θ, Θ_1, Θ_2, and Θ_3 are the contact angles of the glass surface covered by a polymer (Θ), uncovered glass surface (Θ_1), thick polymer film of PI (Θ_2), and thick polymer film of PS (Θ_3); f_1, f_2, and f_3 describe the fractions of the areas uncovered (f_1), covered by PI (f_2), and covered by PS (f_3). If the size of the chemically heterogeneous patches approach molecular or atomic dimensions the modified equation[22] by Israelachvili and Gee can be used:

$$(1 + \cos(\Theta))^2 = f_1 (1 + \cos(\Theta_1))^2 + f_2 (1 + \cos(\Theta_2))^2 + f_3 (1 + \cos(\Theta_3))^2 \quad (2)$$

The contact angles for these surfaces are determined to be $\Theta_1 = 5°$, $\Theta_2 = 77°$, and $\Theta_3 = 90°$. Values of f_1, f_2, f_3 are evaluated due to several approximations.

Approximation 1: In eq 1 we assume that $f_1 \approx \cos(\Theta)$, because $\cos(\Theta_3) = 0$, $\cos(\Theta_1) \approx 1$, $f_1 > f_2$, and $f_1 \cos(\Theta_1) \gg f_2 \cos(\Theta_2)$.

Approximation 2: Wetting of the areas covered by PI does not depend on the amount of grafted PS (see the Results and Discussion. PI Adsorption); because of this, eq 1 can be transformed to

$$\cos(\Theta) = f \cos(\Theta_{PI}) + f_3 \cos(\Theta_3),$$
$$f + f_3 = 1 \quad (3)$$

where Θ_{PI} is the contact angle on the glass plate covered by PI and f is the fraction of the area uncovered with PS.

Approximation 3: This is equal to approximation 2, except for the molecular dimension, where eq 2 is transformed to

$$(1 + \cos(\Theta)^2 = f(1 + \cos(\Theta_{PI})^2 + f_3(1 + \cos(\Theta_2))^2,$$
$$f + f_3 = 1 \quad (4)$$

The corresponding f_i values are calculated and compared for all approximations.

Scanning Probe Microscopy. Because of the softness of the polymer surface, imaging in contact mode is not possible due to large shear forces. Using a new method called PulsedForceMode[23] enables one to map surface topography and adhesion simultaneously without destructive shear forces. In this mode the scan piezo is modulated in the z-direction with a sine function using variable frequencies in the range from 100 Hz up to 5 kHz and variable amplitudes between 10 nm and 1 μm. Because of this, the tip repeatedly moves in and out of contact with the sample surface. A detailed description of this mode is given elsewhere.[23] For our measurements a frequency of 1.5 kHz and modulation amplitudes of about 300 nm have been chosen. As force sensors Si_3N_4 cantilevers with a force constant of 0.9 N m^{-1} have been used.

The quantitative evaluation of the covering morphology has been performed by considering that the structural element has the shape of a spherical segment in order to use the following approach. Using SXMIMAGE software (CSEM company, Switzerland), for every image 10 cross sections are built. For every cross section the height (h_i) and width (a_i) at the base of every peak higher than 1 nm is measured and then average height (h_a) and width (a_a) are calculated. The fraction of the surface covered by the investigated structures is estimated to be $f_3^{SPM} = (\sum s_i)/(a_a l)$, where l is the length of the cross-section, $s_i = \pi a_i^2/4$. The volume of structural elements per unit surface is calculated in the same way to be $v_3^{SPM} = (\sum v_i)/(a_a l)$, where $v_i = \pi\, h_i(h_i^2 + 0.75a_i^2)/6$ is the volume of a spherical segment.

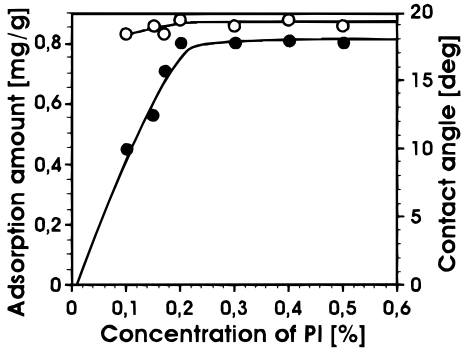

Figure 1. Adsorption (filled symbol) and wetting (unfilled symbol) isotherm for PI adsorbed on the glass surface.

Additionally, the value of the covered surface is determined by software (NIH-image, freeware). All gray-scale SPM images are converted into black-and-white ones. At a definite height corresponding to the base of the surface structure, a threshold can be set. All height values below this threshold are converted into black pixels, height values above are transformed into white pixels. The amount of black and white pixels has been determined as a percentage of the total amount of pixels. Values determined from SPM images are compared to the parameters obtained from contact angle and pyrolysis methods.

Scanning Electron Microscopy. The pictures of grafted PS layers on glass plates were obtained with a ZEISS DSM 962 instrument at 10−20 kV.

Results and Discussion

PI Adsorption. For PI adsorption from the solution in butyl acetate onto glass powder an adsorption isotherm (Figure 1, filled symbols) has been determined by the method of pyrolysis. Additionally, the contact angle values (unfilled symbols) for these specimens are shown. The isotherm shows that, under conditions of PI adsorption onto glass plates prepared for grafting, the PI layer corresponds to a saturated adsorbed layer at plateau area. As it has been obtained before[16] the adsorption amount (A) of PI mainly will be influenced by the solvent nature and is little effected by the substrate nature. Consequently, we may presume that A values for glass and SiO_2 substrate are similar. The A value for PI adsorbed onto a SiO_2 surface has been evaluated[25] by means of null ellipsometry to be on the order of 4 mg/m^2, or in other words, the thickness of the PI adsorbed layer is 4 nm.

Additionally, the low contact angle values show that the adsorbed PI layer is completely permeable for water. The wetting liquid is capable of penetrating through the layer and of being in contact with the substrate. The fraction of the surface covered by PI (f_2) evaluated with eqs 1 and 2 (for $f_3 = 0$) is 0.07 and 0.08, respectively. Consequently, we have to distinguish two notions: (a) the value of the surface coverage—the amount of the polymer in the adsorption layer or coating—and (b) the fraction of the surface capped by adsorbed polymer. One can say that a surface is completely covered by polymer with respect to plateau adsorption amount, but in this case, the surface is not completely capped by polymer, as in our case, with respect to the ability of wetting liquid to penetrate through the layer and reach the substrate.[24] This calculation of f_2 is based on the assumption that the orientations of polar and nonpolar portions in the adsorbed layer are equal to the orientation in thick PI films on the boundary with air and water. The preferable orientation of polar sites to the

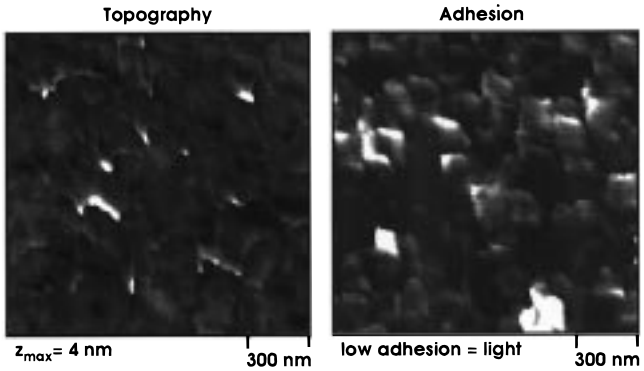

Figure 2. SPM image of a glass surface covered by PI molecules. Whereas in the topographic image no specific structure can be seen, in the adhesion image the glass surface and polymer can be distinguished by different adhesive forces. The glass surface has a lower adhesive force (dark) than the areas covered with polymeric material. *Z* in this and following AFM topography images is the maximum height of the structures.

glass surface should show a higher value of Θ in contrast to the obtained experimental values. In the case of low energy of interaction per segment with the glass substrate, the above-mentioned assumption (about the same orientation in the adsorbed layer and in the thick PI film) could be valid since the surface has not been specially dried to remove strongly adsorbed water. On the other hand, it has been shown by adsorption experiments from PI solution in a solvent (propanol-2 or acetone) containing a definite amount of water (up to 25%) that water will not wash out PI from the glass surface. For all cases the plateau adsorption amount has been found out to be higher than that for adsorption from dry solvent. Consequently, water should change the thermodynamical quality of the solvent, which finally affects the increased adsorption amount. From the data we may presume that a saturated PI adsorption layer is formed by chains stretched in the direction normal to the surface with a very small fraction of attached segments.

To confirm this, we tried to image the PI covered surface by SPM. We were not able to image the topography of the PI adsorbed film onto the glass surface clearly insofar as we could not perform this for the pure glass plate because of the high adhesion between the tip and surface. Whereas in the topographic image (Figure 2a) no specific structure can be seen, in the adhesion image (Figure 2b) pure glass surface and glass covered with polymer can be distinguished by the different adhesive forces. The glass surface has a lower adhesive force than the areas covered with polymeric material. Analyzing the adhesion image shows that the dry adsorbed PI film contains clusters of about 200 nm width. The fraction of area covered with the clusters is substantially larger than the f_2 value calculated from the contact angle. This fact can be explained due to the low density of packing of the chains in the clusters and the low fraction of attached segments per chain.

The fact that there is no substantial difference in wetting of the pure glass surface and the glass surface covered by adsorbed PI allows us to compare the wetting of the grafted PS layers with that of the PI adsorbed layer, assuming that the wetting of areas of the latter is independent of the grafting amount of PS (assumptions 2 and 3 in the Experimental Section).

Grafting. The scheme of the grafting process can be presented as follows:

$$PI \rightarrow R_A^* + R_B^* \quad \text{initiation by adsorbed PI}$$

$$I_B \rightarrow R_B^* \quad \text{initiation in the bulk by additional initiator}$$

$$R_A^* + M \rightarrow R_A^* \quad \text{propagation}$$

$$R_B^* + M \rightarrow R_B^*$$

$$R_A^* + R_B^* \rightarrow P_A \quad \text{termination on the surface}$$

$$R_B^* + R_B^* \rightarrow P_B \quad \text{termination in the bulk}$$

where M is a monomer, I_B is the additional initiator added to the bulk (monomer solution), R_A^* and R_B^* are free radicals attached to the solid substrate and in the bulk, respectively, P_A is the polymer synthesized and attached to the substrate, and P_B is the polymer in the bulk. The most important assumption in this scheme is that the attached free macroradicals terminate in the reaction with the radicals from the bulk, since the termination between two attached radicals is hardly probable.[26] Resulting from this scheme the following kinetic equations can be written:

$$\frac{dR_A^*}{dt} = k_{iA}[PI] - k_t[R_B^*][R_A^*] = 0$$

$$\frac{dR_B^*}{dt} = k_{iB}[I_B] + k_{iA}[PI] - k_t[R_B^*][R_A^*] - k_t[R_B^*]^2 = 0$$

Solving this equation, we obtain expressions for the polymerization on the surface (W_A), in the bulk (W_B) and the degree of polymerization on the surface (Pn_A) and in the bulk (Pn_B):

$$W_A = \frac{k_p}{k_t^{1/2}} \frac{k_{iA}[PI]}{\sqrt{k_{iB}[I_B]}}[M]$$

$$W_B = \frac{k_p}{k_t^{1/2}} \sqrt{k_{iB}[I_B]}[M]$$

$$Pn_A = Pn_B = \frac{k_p}{k_t^{1/2}} \frac{[M]}{\sqrt{k_{iB}[I_B]}}$$

where k_{iA}, k_{iB}, k_p, and k_t are the reaction constants for initiation on the surface, initiation in the bulk, propagation and termination. This equations show that molecular weights of the grafted chains and the chains in the bulk are equal. Whereas the rate of grafting depends on both the initiation rate by PI and I_B, the polymerization in the bulk is effected only by initiation in the bulk. This regularity enables one to keep the molecular weight of grafted chains constant by changing either the temperature of the polymerization or the concentration of the additional initiator in the bulk. The experimental proof of this model is omitted and will be published in the next paper.

We perform the grafting at two temperatures: 90 and 120 °C. To keep the same molecular weight for both experiments of $Pn_A \approx Pn_B \approx 1500$ the concentration of additional initiator I_B is matched (0.1 mol/L and 0.003 mol/L for the experiments at 90 and 120 °C, respectively). The progress of polymerization in terms of the total conversion and amount of the grafted polymer is

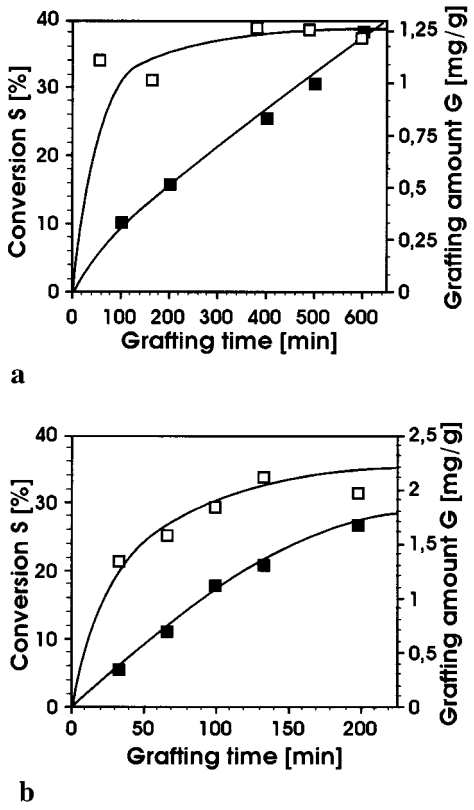

Figure 3. The kinetics of grafting polymerization for grafting at 90 (a) and 120 °C (b). Total conversion in the reaction vessel (*S*, filled symbol) and the amount of the polymer on the surface of the glass substrate (*G*, unfilled symbol) are shown.

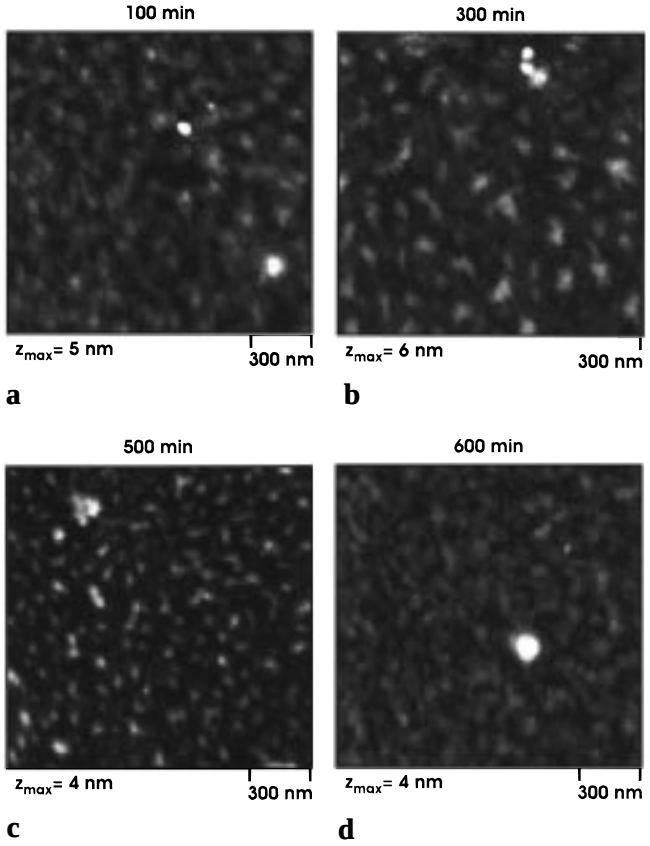

Figure 4. Topography images of glass slides covered with polymer (PS) grafted at 90 °C grafting temperature showing a grain-dimpled structure, where the size of the clusters changes with grafting amount.

shown in Figure 3. For both cases the grafted amount reaches its plateau amount, but the plateau grafted amount at 120 °C is approximately two times higher. If the model is correct, the molecular mass of the grafted chain should be equal in both experiments (MM of the polymer in the bulk in order to GPC was the same for both cases). Consequently the difference in the plateau grafted values can be explained if we assume the multilayer structure of the coating.

Morphology of the Grafting Layers. For the polymerization at 90 and 120 °C images of grafting layers grown at different grafting times are shown in Figure 4a−d and Figure 5a−d. Corresponding contact angles are shown in Tables 1 and 2. On the basis of these values surface fractions covered by PS (f_3) are calculated using the three methods of calculations with approximations 1, 2, and 3 and eqs 1, 3, and 4, respectively. The differences in the calculated values are 3−20%. The modified Cassie equation (eq 4) gives slightly higher values for the fraction of covered surface. Additionally in Tables 1 and 2, surface fractions calculated from SPM images by performing cross sections (f_3^{SPM}) and by the "threshold" method (f_3^{thm}) described in the Experimental Section are presented for both series.

At 90 °C we obtained a lower rate of polymerization and grafting than at 120 °C. The surface covering estimated by contact angle measurements increases slowly, and even after 10 h reaction time no clear limit is reached. The contact angle data show that at the end of the experiment only half of the surface is covered by PS. In contrast, by analyzing the SPM images after 100 minutes grafting time (Figure 4a) about 90% of the surface is covered by PS clusters with average height of 1.6 nm and width 154 nm. The low value of f_3 (about 0.2) determined by contact angle measurements points out that the layer is well permeable for water and only a small fraction of glass surface is screened by PS while the coverage of the surface by clusters is complete (f_3^{SPM} = 0.95). The observed morphology is similar to the dimpled structure predicted by the theory.[11] For PS with Pn = 1500 in Θ solvent the radius of gyration $R_g^{\Theta} = a(M_n/6)^{1/2}$ with a = 0.069 nm[27] is calculated to be 11 nm. Consequently, the radius of the cluster, respectively the distance between dimples, is higher than the R_g^{Θ} value. Due to the theoretical model, this situation corresponds to the regime of high density of grafted chains. A further increasing of the grafting density should create a homogeneous layer. In contrast to this theoretical prediction we observe a more pronounced separation of the film (Figure 4b) during increasing grafting density. This separation is followed by a sharp decrease of f_3^{SPM} = 0.53 whereas f_3 = 0.37 continuously increases. A similar behavior can be observed for the average width of a cluster a_a (Table 1). When the grafting time is prolonged, the values of the fraction of the covered surface evaluated by the contact angle method and SPM become close. The average height of the cluster also increases while the average width and the cluster volume decrease (Figure 4c). In the last image of this series taken after 600 min grafting time (Figure 4d) the increase of clusters width is observed again. This observation can be explained using the data of the "threshold" method (f_3^{thm}). It turned out that very soon after start of the grafting, the second layer has been formed (Table 1).

Table 1. Experimental Data for the Grafted Layer Obtained at 90 °C Grafting Temperature

				f_3^{thm}					
t, min	Θ, deg	f_3: eq 1/eq 3/eq 4	f_3^{SPM}	1 layer	2 layer	a_a, nm	h_a, nm	$v_3^{SPM} \times 10^3$, cm^3/m^2	$G \times 10^3$, g/m^2
100	39.8	0.22/0.19/0.24	0.95	0.89	0.02	154	1.62	0.71	5.55
200	43.2	0.26/0.23/0.29		0.99	0.21				5.05
300	51.9	0.37/0.35/0.42	0.53			135	2.09	0.62	
400	48.4	0.32/0.30/0.36							6.3
500	61.1	0.51/0.49/0.57	0.73	1.00	0.44	126	1.52	0.43	6.25
600	60.3	0.49/0.48/0.56	0.62	1.00	0.89	156	1.43	0.46	6.05

Table 2. Experimental Data for the Grafted Layer Obtained at 120 °C Grafting Temperature

t, min	Θ, deg	f_3: eq 1/eq 3/eq 4	f_3^{SPM}	f_3^{thm} 2 layer	a_a, nm	h_a, nm	$v_3^{SPM} \times 10^3$, cm^3/m^2	$G \times 10^3$, g/m^2
33								6.75
53	57.5	0.45/0.43/0.51	0.42	0.65	188	4.17	1.02	
66	66.1	0.59/0.57/0.65	0.49	0.68	208	4.78	2.17	7.9
99	81.1	0.84/0.81/0.88						9.15
132	79.1	0.81/0.80/0.85	0.65	0.81	237	4.28	1.62	10.6
165	88.5	0.97/0.97/0.98						
198	86.6	0.94/0.94/0.96	0.93	0.95				9.8

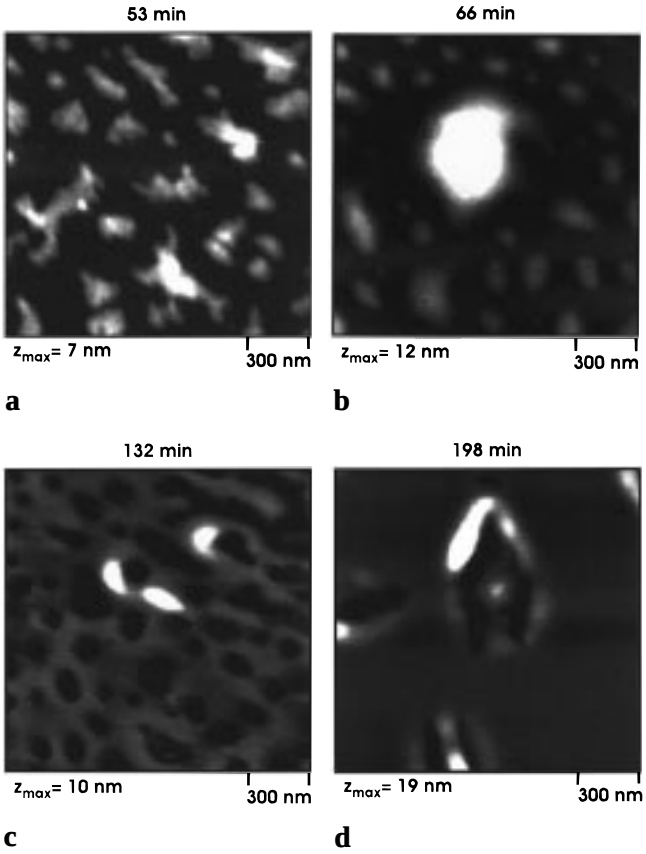

Figure 5. Topography images of glass slides covered with polymer (PS) grafted at 120 °C grafting temperature showing the characteristic changes of the structure depending on the grafting time.

Correlating all data, we may presume the following model for the low temperature grafting: immediately after starting the grafting reaction, a layer consisting of polymeric clusters is formed. This layer is permeable for water. During further grafting this saturated PS layer will not be charged by PS, but due to dewetting phenomena a second layer grows, which is impermeable for water.

At a higher grafting temperature of 120 °C we obtained higher rates of polymerization and grafting (Table 2) even at lower grafting times. In the first SPM image (Figure 5a) taken after 53 min grafting, well-separated large clusters can be seen. Prolonging the grafting time is followed by an increase in cluster width and volume (Figure 5b, Table 2). After 130 min of grafting, the islands start to combine and the transition from an "island" structure to a "lake" structure can be observed (Figure 5c). Determination of the fraction of the covered surface by the grafted polymer from contact angle data and by analyzing SPM images shows a similar increase in the covered fraction. This indicates that in this case the water will not penetrate the grafted layer. Even for the "threshold" method, similar values have been obtained. Consequently, the second layer forms very soon after the start of the polymerization. This can be due to the high rate of grafting. Because of this we immediately obtain a surface covered by grafting polymer.

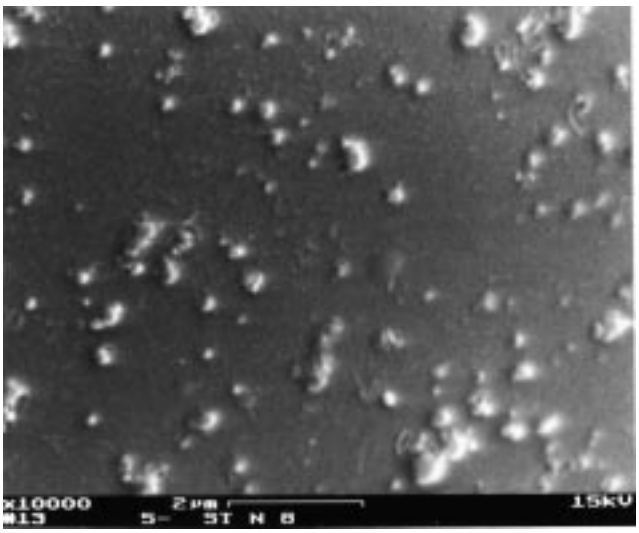

Figure 6. SEM image of the PS coating on the glass surface, which corresponds to a plateau grafting amount at 120 °C.

After long grafting times, the coalescence of clusters results in a homogeneous layer with numerous big craterlike features (Figure 5d). These structures can also be observed very well by means of scanning electron microscopy (Figure 6). We presumed that these big aggregates are due to an overshot polymer insoluble in the solvent due to cross-links. The cross-linked structures we observed earlier[17] were explained by pronounced chain transfer reactions in thick grafted polymer layer. Microscopic size contamination (dust) can also promote the formation of the big clusters. The values for the grafting amount (v_3^{spm}) in Table 2 are

calculated without consideration of these big aggregates. Because of this, the values are smaller than expected.

Comparing the amount of grafted polymer determined by the pyrolysis method to the values estimated by other methods, we observed that a substantially higher value for the pyrolysis method than that evaluated from cross section measurements for all series of the experiments has been found. Because contact angle measurements or SPM investigations are mainly surface sensitive, we obtained the grafting amount only for the top layer. The higher values obtained from the pyrolysis experiments are an evidence for the growth of a multilayer structure. Besides, a large amount of grafted polymer can be accumulated in aggregates (Figure 6).

The results obtained for the above-mentioned two series allowed us to follow the grafting process at different fractions of the occupied surface. In the first step, the surface is covered by grafted chains. However, very soon after starting this process the layer becomes saturated. When the sample is rinsed with solvent, the ungrafted polymer is washed out and the dry grafted layer is allowed to form the cluster structures by phase separation of collapsed chains. We observe a dimpled surface in good agreement with the theoretical prediction. During further grafting a more heterogeneous layer is formed. This is in contrast to the theory, where grafted chains considered to be strongly adhered to the substrate and homogeneous layers will be formed. To explain the formation of the heterogeneous polymer covering with different scales of heterogeneity, we propose the following model. In our case the grafted chains are attached by means of physisorption of short PI blocks. This reversible bonding enables them to move along the surface. Because of this, at a large grafting density the transition from the dimpled structure to the force out regime, where a second layer begins to form, is possible. During in situ grafting, free chains (ungrafted) and grafted polymer are simultaneously synthesized. So, grafted polymer chains are stretched not only due to the competition between adjacent chains but also because of the swelling by ungrafted polymer. Such conditions of the overshoot phenomena in a swelled layer can be reached in a relatively short time of grafting. The formation of overshoot structures enhances the following polymerization in this structures such as in the polymer gel with possible partial crosslinking of chains. This also accelerates the growth of the clusters.

Another factor which determines the thickness of the coating is a ratio between the rate of polymerization and washing out of the chains from the layer. The plateau amount of grafted polymer is higher at a higher rate of grafting. A very slow diffusion of a chain in the polystyrene brush was also observed by Klein et al.[28]

Conclusion. To follow the grafting process with an additional investigation of the morphology of grafted layers, the contact angle method and SPM techniques can be used supplementarily. The in situ grafting of PS on a glass surface permits one to reach the maximum density of grafted brushes. Because of the rinsing procedure, ungrafted polymer is washed out. The dried grafted layer forms cluster structures by phase separation of collapsed chains. The results obtained mainly from SPM images show several interesting facts: (1) At the grafting density regime, where the theory proposes a homogeneous layer, island structures of grafted polymer with a size substantially higher than can be predicted by the theory are formed. (2) Only due to the grafting can in situ overshot polymer structures of large sizes grow. Analyzing contact angle data and SPM images determines that (3) the amount of grafted polymer is substantially higher than can be expected from the conception of monolayer covering. (4) The substrate surface is covered by grafted polystyrene at a very high amount of grafted polymer.

Correlating data obtained by different methods of analyzing the SPM with data estimated by contact angle measurements and grafting amount evaluations, we suggest a mechanism for the grafting process which included at least three stages: (1) formation of a brushlike polymer layer; (2) growth of a second layer of ungrafted chains in the regime when excess chains are forced out from the first layer; (3) creation of polymer clusters up to 100−200 nm diameter due to the gel polymerization in the clusters, formed in the force out regime.

Acknowledgment. We thank Armin Rosa-Zeiser, Bernd Zink, and Martin Quintus for performing SPM measurements. We are gratefully acknowledge the NATO Scientific and Environmental Affairs Division for the support by providing a Linkage Grants under HTECH.LG 940579, 961267, and the Sonderforschungsbereich 239 of the Deutsche Forschungsgemeinschaft (DFG). S.M. thanks the Alexander von Humboldt Foundation for the support of this work. We acknowledge a stimulating discussion with Dr. M. Stamm (MPI Mainz). The authors thank CSEM Company (Switzerland) for providing the SXMIMAGE software.

References and Notes

(1) Milner, S. T. *Science* **1991**, *251*, 905.
(2) Halperin, A.; Tirel, M.; Lodge, T. P. *Adv. Polym. Sci.* **1992**, *100*, 31.
(3) Fleer, G. J.; Cohen Stuart, M. A.; Scheutjens, J. M. H. M.; Cosgrove, T.; Vincent, B. *Polymer at Interface*; Chapman and Hall: London, 1993.
(4) *Long and Short Chains at Interface*; Dailland, J., et al., Eds.; Editions Frontieres: Gif-sur-Yvette, France, 1995.
(5) Kawaguchi, M.; Takahashi, A. *Adv. Colloid Interface Sci.* **1992**, *37*, 219.
(6) Overney, R. M.; Leta, D. P.; Pictorski, C. F.; Rafailovich, M. H.; Liu, Y.; Quinn, J.; Sokolov, J.; Eisenberg, A.; Overney, G. *Phys. Rev. Lett.* **1996**, *76*, 1272.
(7) Koutsos, V.; van der Vegte, E. W.; Pelletier, E.; Stamouli, A.; Hadziioannou, G. *Macromolecules* **1997**, *30*, 4719.
(8) Uchida, E.; Ikada, Y. *Macromolecules* **1997**, *30*, 5464.
(9) Spatz, J. P.; Möller, M.; Noeske, M.; Behn, R. J.; Pietralla, M. *Macromolecules* **1997**, *30*, 3874.
(10) Duchet, J.; Chapel, J.-P.; Chabret, B.; Spitz, R.; Gerard, J.-F. *J. Appl. Polym. Sci.* **1997**, *65*, 2481.
(11) Yeung, C.; Balazs, A. C.; Jasnow, D. *Macromolecules* **1993**, *26*, 1914.
(12) Tang, H.; Szleifer, I. *Europhys. Lett.* **1994**, *28*, 19.
(13) Siqueira, D. F.; Köhler, K.; Stamm, M. *Langmuir* **1995**, *11*, 3092.
(14) Reiter, G., Auroy, P., Auvray, L. *Macromolecules* **1996**, *29*, 2150.
(15) Henn, G.; Bucknall, D. G.; Stamm, M.; Vanhoorne, P.; Jerome, R. *Macromolecules* **1996**, *29*, 4305.
(16) Minko, S. S.; Luzinov, I. A.; Evchuk, I. Yu.; Voronov, S. A. *Polymer* **1996**, *37*, 177.
(17) Luzinov; I. A.; Evchuk; I. Yu; Minko; S. S.; Voronov; S. A. *J. Appl. Polym. Sci.* **1998**, *67*, 299.
(18) Luzinov, I.; Voronov, A.; Minko, S.; Kraus, R.; Wilke, W.; Zhuk, A. *J. Appl. Polym. Sci.* **1996**, *61*, 1101.
(19) Cassie, A. B. D.; Baxter, S. *Trans. Faraday Soc.* **1944**, *40*, 546.
(20) Cassie, A. B. D. *Discuss. Faraday Soc.* **1948**, *3*, 11.

(21) Cassie, A. B. D. *Discuss. Faraday Soc.* **1952**, *75*, 5041.
(22) Israelachvili, J. N.; Gee, M. L. *Langmuir* **1989**, *5*, 288.
(23) Rosa, A.; Weilandt, E.; Hild, S.; Marti, O. *Meas. Sci. Technol.* **1997**, *8*, 1.
(24) Minko; S. S.; Luzinov; I. A.; Voronov; A. S. *Colloid J.* **1994**, *56*, 720.
(25) Erb, V.; Stamm, M.; Voronov, A.; Luzinov, I.; Minko, S. Unpublished results.
(26) Minko, S. S.; Sidorenko, A. A.; Voronov, S. A. *Polym. Sci., Ser. B* **1995**, *37*, 401.
(27) *Polymer Handbook*; Brandrup, J.; Immergut, E. H., Eds.; Wiley-Interscience Publication: USA, 1975.
(28) Tauton, H. J.; Toprakcioglu, C.; Fetters, L. J.; Klein, J. *Macromolecules* **1990**, *23*, 571.

MA971413W